Breviscapine alleviates podocyte injury by inhibiting NF-κB/NLRP3-mediated pyroptosis in diabetic nephropathy

Linlin Sun [Corresp., 1], **Miao Ding** [1], **Fuhua Chen** [1], **Dingyu Zhu** [1], **Xinmiao Xie** [1]

[1] Department of Nephrology, Tongren Hospital Shanghai Jiaotong University School of Medicine, shanghai, China

Corresponding Author: Linlin Sun
Email address: llsunzj@sina.com

Podocyte injury is a critical factor in the pathogenesis of diabeticnephropathy (DN). Emerging evidence has demonstrated that breviscapine (Bre) exerts a renoprotective effect on diabetic rats. However, the effects of Bre on regulating podocyte injury under high glucose (HG) conditions remain unclear. In this study, an experimental mouse model of DN was induced by intraperitoneal injections of streptozotocin (STZ) *in vivo*. The effects of Bre on podocyte injury were assessed using cell counting kit-8 (CCK-8) assay, TdT-mediated dUTPnick-endlabelling(TUNEL) staining, quantitative real-time PCR (qRT–PCR) and western blot analysis. We found that renal function was significantly decreased in diabetic mice, and this effect was blocked by Bre treatment. Bre effectively increased podocyte viability and inhibited HG-induced cell apoptosis. Furthermore, Bre ameliorated HG-induced podocyte injury , as evidenced by decreased α-smooth muscle actin (α-SMA) expression and increased podocin and synaptopodin expression. Mechanistically, Bre inhibited HG-induced nuclear factorkappaB(NF-κB) signalling activation and subsequently decreased NLR family pyrin domain containing 3 (NLRP3) inflammasome activation, resulting in a decrease in pyroptosis. Pharmacological inhibition of NLRP3 decreased HG-induced podocyte injury, whereas the NLRP3 agonist abrogated the effects of Bre on inhibiting podocyte injury. In summary, these results demonstrate that Bre alleviates HG-induced podocyte injury and improves renal function in diabetic mice, at least in part by inhibiting NF-κB/NLRP3-mediated pyroptosis.

1 **Breviscapine alleviates podocyte injury by inhibiting NF-κB/NLRP3-**

2 **mediated pyroptosis in diabetic nephropathy**

4 Linlin Sun*, Miao Ding, Fuhua Chen, Dingyu Zhu, Xinmiao Xie

6 Department of Nephrology, Tongren Hospital, Shanghai Jiao Tong University School of

7 Medicine, Shanghai, China.

9 *Corresponding author: Dr Linlin Sun

10 **Dr Linlin Sun**: Department of Nephrology, Tongren Hospital, Shanghai Jiao Tong University

11 School of Medicine, 1111 Xianxia Road, Shanghai, China, 200336. Email: llsunzj@sina.com.

12 Tel 86-18017337095. Fax 021-52039999.

14 **Running title:** Breviscapine alleviates podocyte injury.

Abstract

Podocyte injury is a critical factor in the pathogenesis of diabetic nephropathy (DN). Emerging

evidence has demonstrated that breviscapine (Bre) exerts a renoprotective effect on diabetic rats.

However, the effects of Bre on regulating podocyte injury under high glucose (HG) conditions

remain unclear. In this study, an experimental mouse model of DN was induced by

intraperitoneal injections of streptozotocin (STZ) *in vivo*. The effects of Bre on podocyte injury

were assessed using cell counting kit-8 (CCK-8) assay, TdT-mediated dUTP nick-

end labelling (TUNEL) staining, quantitative real-time PCR (qRT–PCR) and western blot

analysis. We found that renal function was significantly decreased in diabetic mice, and this

effect was blocked by Bre treatment. Bre effectively increased podocyte viability and inhibited

HG-induced cell apoptosis. Furthermore, Bre ameliorated HG-induced podocyte injury, as

evidenced by decreased α-smooth muscle actin (α-SMA) expression and increased podocin and

synaptopodin expression. Mechanistically, Bre inhibited HG-induced nuclear

factor kappa B (NF-κB) signalling activation and subsequently decreased NLR family pyrin

domain containing 3 (NLRP3) inflammasome activation, resulting in a decrease in pyroptosis.

Pharmacological inhibition of NLRP3 decreased HG-induced podocyte injury, whereas the

NLRP3 agonist abrogated the effects of Bre on inhibiting podocyte injury. In summary, these

results demonstrate that Bre alleviates HG-induced podocyte injury and improves renal function

in diabetic mice, at least in part by inhibiting NF-κB/NLRP3-mediated pyroptosis.

Keywords: Diabetic nephropathy, podocyte, breviscapine, NLRP3, pyroptosis.

1. Introduction

Diabetic nephropathy (DN) is a serious diabetic microvascular complication that occurs in up to 20-50% of individuals with diabetes (Alicic et al. 2017; Selby & Taal 2020). The morphological alterations in glomeruli and tubules caused by podocyte injury and excessive mesangial cell proliferation are the two major characteristics of DN (Nagata 2016; Rousseau et al. 2022; Thomas & Ford Versypt 2022). In addition to controlling blood glucose and blood pressure, blocking the renin-angiotensin-aldosterone system is a therapeutic option for DN (Sawaf et al. 2022). However, these treatments cannot reverse this disease. It is critical to uncover the underlying mechanisms of podocyte injury to develop an effective therapy.

Podocytes, which are glomerular visceral epithelial cells, are essential components of the renal filtration barrier that create slit diaphragms within the glomeruli (Shankland 2006; Yan et al. 2022). Mounting evidence has shown that podocyte injury is an early and critical event in the pathogenesis of DN (Asanuma 2015; Nagata 2016; Yasuno et al. 2010). Hyperglycaemia leads to podocyte injury through various pathways, including inflammation, reactive oxygen species (ROS), and endoplasmic reticulum stress (Schena & Gesualdo 2005; Wolf 2004). These factors result in podocyte apoptosis, aberrant expression of interconnecting slit diaphragm proteins (nephrin and podocin), and cytoskeletal rearrangement in podocytes (El-Aouni et al. 2006; Jefferson et al. 2008).

Intracellular inflammation can be activated by various stimuli and is a typical mechanism by which podocyte damage occurs (Wang et al. 2022a). The NLRP3 inflammasome has critical effects on the production of proinflammatory cytokines, and is closely correlated with podocyte

57   damage and DN (Jiang et al. 2021; Xu et al. 2021; Zhang et al. 2022a). NLRP3 inflammasome

58   activation in podocytes accelerates kidney injury in DN (Shahzad et al. 2022), whereas CY-09, a

59   specific NLRP3 inflammasome antagonist, alleviates renal damage in DN by repressing NLRP3

60   activation (Yang & Zhao 2022). Moreover, NLRP3 inflammasome-induced pyroptosis is a new

61   form of cell death associated with podocyte injury (Lin et al. 2020). As an intracellular pattern

62   recognition receptor (PRR), NLRP3 can be activated by many pathogen-associated molecular

63   patterns (PAMPs) and damage-associated molecular patterns (DAMPs). Subsequently, NLRP3

64   assembles with the adaptor ASC (apoptosis-associated speck-like protein) and pro-caspase-1,

65   resulting in ASC oligomerization and caspase-1 activation. Active caspase-1 catalyses IL-18 and

66   IL-1β maturation (Lasithiotaki et al. 2018; Peng et al. 2020) and cleaves gasdermin D (GSDMD)

67   into the N-terminal (GSDMD-N) and C-terminal (GSDMD-C) forms (Ding et al. 2016; Latz et al.

68   2013). GSDMD-N forms pores in the cell membrane and mediates perforation, which results in

69   pyroptosis and proinflammatory factor release (Shi et al. 2015). Pharmacological inhibition of

70   NLRP3-mediated pyroptosis can effectively alleviate podocyte injury in DN (Feng et al. 2021;

71   Wang et al. 2022a; Zhang et al. 2022a).

72   Breviscapine (Bre), a flavonoid extract from *Erigeron breviscapus*, exerts renoprotective effects

73   on diabetic rats. Bre treatment decreases albuminuria and alleviates glomerular hypertrophy and

74   tubulointerstitial injury (Qi et al. 2006; Xu et al. 2013). Bre alleviates renal fibrosis and contrast

75   medium-induced nephropathy (Jiang et al. 2016). Based on above findings, we speculated

76   whether Bre relieves HG-induced podocyte injury and improves renal function in diabetic mice

77   by regulating NLRP3 inflammasome.

78

2. Materials and Methods

2.1. Animal model

This work was performed with the approval of the Animal Ethics Committee of Shanghai Jiao

Tong University Affiliated Tong Ren Hospital (No. 2019-060) according to the ARRIVE

guidelines to minimize animal suffering (Percie du Sert et al. 2020). Male C57BL/6J wild-type

mice (approximately 8 weeks old) were purchased from Shanghai Regan Biotechnology

(Shanghai, China), housed in a thermostatic room (25±2 °C) with 12/12 light/dark cycles,

and given free access to chow and water. The mice were randomly divided into three groups

(n=7): control group, diabetic group, and Bre-treated group. Diabetes was induced by

intraperitoneal (i.p.) injections of STZ (Aladdin, Shanghai, China) at a dose of 50 mg/kg for 5

consecutive days, as previously described (Lee et al. 2022; Song et al. 2022; Zhong et al. 2019).

Mice with blood glucose > 16.7 mmol/L were considered diabetic 3 days after the injection (He

et al. 2013). Based on the previous studies (Jiang et al. 2016; Lan et al. 2022) and our

preliminary experiments, diabetic mice in the Bre-treated group were administered Bre daily by

oral gavage at a dose of 15 or 30 mg/kg for 4 weeks. Bre was purchased from Shanghai Winherb

Medical Science Co., Ltd., (Shanghai, China). Control mice were i.p. administered sodium

citrate buffer. After being treated, all mice were euthanized by cervical dislocation under deep

anaesthesia (pentobarbital sodium, 40 mg/kg), and renal tissues and blood samples were

collected to carry out biochemical and pathological assessments, respectively. The establishment

of diabetic mice model and treatment procedure were displayed in Figure 1A. In this study,

99   animals suffering from unexpected disease were euthanized as described previously.

2.2.   Cell culture and treatments

101   The immortalized mouse podocyte line MPC5 was purchased from the Cell Bank of the Chinese

102   Academy of Sciences (Shanghai, China). To induce differentiation, MPC5 podocytes were

103   cultured in RPMI-1640 medium (Gibco, NY, USA) supplemented with 10% FBS (Gibco)

104   without IFN-γ for two weeks in a 5% CO_2 incubator (Liu et al. 2016a). Differentiated MPC5

105   cells were used in subsequent experiments. MPC5 cells were treated with HG (30 mM) to

106   establish an *in vitro* DN model, and 5 mM glucose was used as a control (low glucose). To

107   examine the effects of Bre, MCC950, nigericin, and Ac-YVAD-cmk on MPC5 cell injury, the

108   cells were treated with 50 μM or 100 μM Bre, 10 μM MCC950 (Merck, MA, USA), 10 μM

109   nigericin (MCE, NJ, USA), and 40 μM Ac-YVAD-cmk (Merck), and then cell injury was

110   assessed.

2.3.   qRT–PCR

112   Total RNA was isolated from MPC5 cells or renal tissues with TRIzol reagent (TaKaRa, Tokyo,

113   Japan), quantified using a Nanodrop (Thermo Fisher Scientific, MA, USA), and then used to

114   synthesize first-strand cDNA using M-MLV (TaKaRa) in a final volume of 20 μl. qRT–PCR was

115   performed in triplicate using KAPA SYBR® FAST (Roche, Basel, Switzerland) on a Bio-Rad

116   CFX96 qPCR System (CA, USA) under the following conditions: 94 °C for 10 min, followed by

117   38 cycles (94 °C for 15 s and 59 °C for 15 s). Gene expression was calculated using the $2^{(-\Delta\Delta CT)}$

118   method after normalization to β-actin (Livak & Schmittgen 2001). All primers are shown in

119   Supplementary Table S1.

120 **2.4. CCK-8 assay**

121 MPC5 cells were cultured in 96-well plates (3000 cells per well) and treated with HG and other

122 reagents (50 or 100 μM Bre, 10 μM MCC950, or 40 μM Ac-YVAD-cmk). Forty-eight hours

123 later, the cells were treated with CCK-8 (10 μL, Abcam, CA, USA) for 1 h, and then the

124 absorbance was measured at 450 nm with a microplate reader (Bio-Rad).

125 **2.5. Western blot analysis**

126 Total protein was isolated from MPC5 cells using RIPA buffer (Thermo Fisher Scientific) and

127 quantitated using a BCA protein quantification kit (Abcam), and the proteins were separated via

128 10% SDS–PAGE. Then, the proteins were transferred to PVDF membranes (Roche). After being

129 sealed with 5% nonfat milk and washed three times with TBST, the membranes were incubated

130 with primary antibodies against Bax (1:1500, ab182733, Abcam), Bcl-2 (1:2000, ab182858,

131 Abcam), α-SMA (1:400, MA5-14084, Thermo Fisher Scientific), podocin (1:800, PA5-79757,

132 Thermo Fisher Scientific), synaptopodin (1:1000, ab259976, Abcam), p-p65 (1:800, MA5-

133 15160), NLRP3 (1:800, ab263899), cleaved caspase-1 (1:1000, PA5-99390, Thermo Fisher

134 Scientific), GSDMD (1:900, ab209845, Abcam), and β-actin (1:8000, MA1-140, Thermo Fisher

135 Scientific) for 1 h at room temperature. After being washed three times with TBST, the

136 membranes were incubated with HRP-conjugated secondary antibodies (1:7000) for 1 h, and

137 then the immunoblots were visualized using an ECL kit (Roche) and quantitated using ImageJ

138 software (Bethesda, MA, USA).

139 **2.6. IF analysis**

140 MPC5 cells were fixed with 4% PFA for 15 min, permeabilized with 0.5% Triton X-100 for 25

141 min, sealed with normal donkey serum for 60 min, and then incubated with primary antibodies

142 against α-SMA (1:100, MA5-14084, Thermo Fisher Scientific), synaptopodin (1:100, ab259976,

143 Abcam), and p65 (1:300, ab32536, Abcam) overnight at 4 °C. After being washed three

144 times with PBST, the slides were incubated with goat anti-rabbit antibodies (1:1500, A27039,

145 Invitrogen) for 2 h in the dark. Nuclei were visualized by staining with DAPI (Solarbio,

146 Shanghai, China). Images were obtained using a DMI4000B fluorescence microscope (Leica,

147 Wetzlar, Germany).

148 **2.7. TUNEL assay**

149 MPC5 cells were treated with HG and other reagents (50 or 100 μM Bre, 10 μM MCC950, or 40

150 μM Ac-YVAD-cmk) for 48 h and then subjected to TUNEL staining (Solarbio) to assess

151 apoptosis. TUNEL-positive cells were observed with a DMI4000B fluorescence microscope.

152 **2.8. Serum creatinine and blood urea nitrogen (BUN) levels**

153 Serum samples were collected, and serum creatinine and BUN levels were measured with an

154 automated biochemical analyser (PUZS-600A/B, PERLONG, Beijing, China).

155 **2.9. Histological analysis**

156 Renal tissues were collected, fixed with 4% PFA, embedded in paraffin, and cut into 4 μm-thick

157 sections. The sections were stained with haematoxylin and eosin (H&E), periodic-acid-Schiff

158 (PAS), and Masson's trichrome by staining kits in accordance with the manufacturer's

159 instructions (Solarbio).

160 **2.10. LDH assay**

161 LDH was measured using an LDH assay kit (ab65393, Abcam). The absorbance was measured at

162 450 nm with a microplate reader (Bio-Tek, USA).

163 **2.11. Statistical analysis**

164 The data are displayed as the mean ± SD from at least three independent replicates and analysed

165 using SPSS 20 software (IBM, NY, USA). Student's *t* test was used for intergroup comparisons

166 and one-way ANOVA (Scheffé test) was used for multi-group comparison. Data were

167 considered statistically significant when the *P* value was less than 0.05.

168

169 **3. Results**

170 **3.1. Bre decreased glomerular injury in DN mice**

171 To investigate the effect of Bre on the regulation of renal function in DN mice, the mice were i.p.

172 injected with STZ and then treated with Bre by intragastric administration. As shown in Figure

173 1B and C, the glomerular surface area was prominently increased in DN mice, whereas Bre

174 treatment effectively inhibited this increase. PAS and Masson staining revealed the proliferation

175 of the mesangial matrix and glomerular fibrosis in DN mice, and these effects were reversed by

176 Bre (Figure 1D and E). Serum creatinine and BUN levels, which are known biomarkers of renal

177 function, were further assessed after treatment with Bre. Figure 1F and G show that serum

178 creatinine and BUN levels were significantly elevated in DN mice, and these effects were

179 blocked by Bre treatment. These results demonstrate that Bre alleviates glomerular injury in DN

180 mice.

181 **3.2. Bre decreased HG-induced podocyte apoptosis *in vitro***

182 Then, the effects of Bre on the regulation of podocyte viability and apoptosis were assessed *in*

183   *vitro*. Figure 2A shows that podocyte viability was significantly decreased after HG treatment,

184   and Bre effectively restored cell viability in a dose-dependent manner. The results of TUNEL

185   staining showed that HG induced marked podocyte apoptosis, and these effects were reversed by

186   Bre (Figure 2B and C). Furthermore, there was a significant increase in Bax protein expression

187   and a reduction in Bcl-2 protein expression in podocytes under HG conditions compared with the

188   low glucose control, and these effects were blocked by Bre (Figure 2D). Bre treatment also

189   inhibited HG-induced increase in reactive oxygen species (ROS) levels in podocytes (Figure 2E).

190   **3.3.   Bre decreased HG-induced podocyte injury *in vitro***

191   The biological roles of Bre in regulating HG-induced podocyte injury were next evaluated by

192   assessing α-SMA, podocin, and synaptopodin expression in podocytes. As shown in Figure 3A,

193   α-SMA mRNA levels were markedly elevated, and podocin and synaptopodin mRNA levels

194   were downregulated under HG conditions compared with the low glucose control; these changes

195   were significantly blocked by Bre treatment. Consistent with the qRT–PCR results, western blot

196   analysis revealed similar effects of Bre on the regulation of α-SMA, podocin, and synaptopodin

197   protein expression in HG-treated podocytes (Figure 3B and C). IF staining revealed that HG

198   treatment increased α-SMA levels and decreased synaptopodin levels in podocytes, while Bre

199   effectively inhibited these changes (Figure 3D). These data demonstrate that Bre alleviates HG-

200   induced podocyte injury *in vitro*.

201   **3.4. Bre decreased NF-κB/NLRP3-mediated pyroptosis in HG-treated podocytes *in vitro***

202   Given the crucial role of NF-κB signalling and NF-κB-mediated NLRP3 inflammasome

203   activation in podocyte injury (Ke et al. 2021; Lv et al. 2022; Xu et al. 2021), the effects of Bre on

204   the regulation of NF-κB/NLRP3 signalling activation in podocytes were next investigated.

205   Podocytes were treated with HG and Bre, and then phosphorylated p65 (p-p65) levels were

206   assessed by western blot analysis. Figure 4A and B show that p-p65 levels were markedly

207   increased in podocytes under HG stress, and these effects were significantly reversed by Bre,

208   indicating that Bre could inhibit HG-induced NF-κB activation. To further verify this hypothesis,

209   nuclear translocation of p65 was assayed in podocytes treated with HG and Bre. Figure 4C

210   shows that Bre suppressed HG-induced p65 nuclear translocation in podocytes. Furthermore,

211   NLRP3 and activated caspase-1 protein levels were prominently increased in podocytes under

212   HG conditions compared with the control, and Bre alleviated HG-induced NLRP3

213   inflammasome activation (Figure 4D and E). Thus, Bre further decreased the HG-induced release

214   of IL-18 and IL-1β (Figure 4F). Bre also reduced HG-induced IL-1β production in cell

215   supernatant after treatment with Bre (Supporting Figure S1). Subsequently, NLRP3-mediated

216   pyroptosis in HG-treated podocytes was investigated by assessing GSDMD cleavage and LDH

217   release. As expected, HG treatment resulted in obvious cleavage of GSDMD and elevated levels

218   of the GSDMD-N fragment in podocytes, and these changes were blocked by Bre (Figure 4G).

219   Bre also decreased the HG-induced release of LDH (Figure 4H). These data suggest that Bre

220   alleviates NF-κB/NLRP3-mediated pyroptosis in HG-treated podocytes.

221   **3.5. Bre decreased podocyte injury by inhibiting NLRP3-mediated pyroptosis *in vitro***

222   The role of NLRP3-mediated pyroptosis in podocyte injury was next investigated using MCC950

223   (NLRP3 inhibitor) (Tang et al. 2020), Ac-YVAD-CMK (caspase-1 inhibitor) (Wang et al.

224   2022b), and nigericin (NLRP3 activator) (Jian et al. 2020; Mo et al. 2021). Podocytes were

225   treated with HG in the presence or absence of MCC950, Ac-YVAD-CMK, or nigericin, and then

226   podocyte injury was evaluated. HG treatment caused a prominent decrease in podocyte viability,

227   and these effects were reversed by MCC950 or Ac-YVAD-CMK (Figure 5A). MCC950 or Ac-

228   YVAD-CMK decreased α-SMA levels and increased synaptopodin levels in HG-treated

229   podocytes (Figure 5B), indicating that NLRP3-mediated pyroptosis exerted crucial effects on

230   HG-induced podocyte injury. To further examine whether Bre alleviated podocyte injury by

231   inhibiting NLRP3 inflammasome activation, podocytes were treated with HG plus Bre in the

232   presence or absence of nigericin, and podocyte injury was evaluated. Figure 5C-E shows that

233   compared with the vehicle, nigericin increased α-SMA expression and decreased synaptopodin

234   expression at the mRNA and protein levels in the presence of HG plus Bre. IF staining revealed

235   similar results (Figure 5F).

236   **3.6. Bre inhibited NLRP3 activation and decreased podocyte injury in the renal tissues of**

237   **DN mice**

238   Finally, the effects of Bre on inhibiting NLRP3 activation and decreasing podocyte injury were

239   assessed in the renal tissues of DN mice. The IHC results revealed that synaptopodin expression

240   was decreased in the renal tissues of DN mice, and this effect was reversed by Bre (Figure 6A).

241   Moreover, α-SMA levels were increased and podocin levels were decreased in DN mice, and

242   these alterations were blocked by Bre (Figure 6B). The IHC results further revealed that NLRP3

243   expression was elevated in the renal tissues of DN mice, and Bre effectively inhibited this

244   increase (Figure 6C). As a result, Bre attenuated proinflammatory cytokine production in the

245   renal tissues of DN mice (Figure 6D).

246

4.   Discussion

248   The pathogenesis of DN is extremely complicated   and   poorly understood.   The   conventional

249   treatment for early DN generally involves lowering blood sugar and blood pressure and blocking

250   the RAAS (Chang et al. 2020; Choudhury et al. 2010). Unfortunately, DN frequently progresses

251   into glomerulosclerosis, kidney fibrosis, and ESRD (Dong et al. 2022). Given the renoprotective

252   roles of Bre in diabetic mice, we investigated whether Bre exerts its renoprotective effects by

253   alleviating HG-induced podocyte injury. We demonstrated that i) Bre alleviated glomerular

254   injury in DN mice, ii) Bre alleviated HG-induced podocyte apoptosis and podocyte injury, iii)

255   Bre alleviated NF-κB/NLRP3-mediated pyroptosis in HG-treated podocytes, and iv) Bre

256   alleviated HG-induced podocyte injury by inhibiting NLRP3-mediated pyroptosis.

257   Recent studies have revealed the protective effects of Bre against renal injury (Liu et al. 2016b),

258   cerebral ischaemia–reperfusion injury (Chen et al. 2022), liver injury (Lan et al. 2022; Liu et al.

259   2018), and myocardial damage (Wang et al. 2009) through various mechanisms, such as

260   inflammation, ROS production, and endoplasmic reticulum stress (Schena & Gesualdo 2005;

261   Wolf 2004). Although inflammation is a protective response to infection and tissue injury, an

262   excessive inflammatory response results in long-lasting tissue injury (Liu et al. 2017). NF-κB

263   plays a critical role in orchestrating multiple aspects of the inflammatory response. Furthermore,

264   NF-κB signalling is an inevitable prerequisite for the activation of the NLRP3 inflammasome

265   (Boaru et al. 2015), which has vital effects on the production of proinflammatory cytokines and

266   the initiation of pyroptosis (Yu et al. 2022). Emerging evidence has demonstrated that various

267   active components derived from traditional Chinese herbal medicines exhibit renoprotective

268   effects by inhibiting the NLRP3 inflammasome. Fucoidan, an active component in *Laminaria*

269   *japonica*, attenuates renal fibrosis by inhibiting NLRP3-dependent pyroptosis in podocytes

270   (Wang et al. 2022a). As a natural dietary flavonoid in various fruits, fisetin alleviates podocyte

271   injury in DN mice by inhibiting NLRP3 inflammasome activation (Dong et al. 2022). Bre is a

272   flavonoid extract from *Erigeron breviscapus* and exerts renoprotective effects on diabetic rats

273   (Qi et al. 2006; Xu et al. 2013). Here, the role of Bre in regulating podocyte injury in DN mice

274   was further investigated. We demonstrated that Bre improved renal function in diabetic mice.

275   Furthermore, Bre increased podocyte viability and decreased HG-induced podocyte apoptosis

276   and injury. Mechanistically, Bre attenuated HG-induced NF-κB/NLRP3 activation, resulting in

277   decreased podocyte pyroptosis.

278   Although the role of Bre in inhibiting NLRP3 inflammasome activation has been revealed,

279   additional mechanistic studies are necessary to provide further insights into the underlying

280   mechanisms by which Bre inhibits NLRP3 activation. Bre possesses antioxidant

281   activities (Zhang et al. 2022b), and ROS are crucial for triggering NLRP3 inflammasome

282   formation and activation (Tschopp & Schroder 2010). Therefore, it would be worthwhile to

283   examine whether Bre represses NLRP3 activation in a ROS-dependent manner, as well as NF-κB

284   signalling. In addition, podocyte injury and excessive mesangial cell proliferation are the two

285   major characteristics of DN (Nagata 2016; Rousseau et al. 2022; Thomas & Ford Versypt 2022).

286   It is important to investigate whether Bre regulates NLRP3 activation in mesangial cells in

287   addition to podocytes. **Conclusion**: Bre alleviates HG-induced podocyte injury by inhibiting NF-

288   κB/NLRP3-mediated pyroptosis in DN mice.

289

Ethics approval

291   This work was performed with the approval of the Animal Ethics Committee of Shanghai Jiao

292   Tong University Affiliated Tong Ren Hospital (No. 2019-060).

Data accessibility

294   The following information was supplied regarding data availability. The raw measurements,

295   figures and images are available in the Supplemental Files.

Author contributions

297   All authors conceived and designed the experiments, performed the experiments, analysed the

298   data, prepared the figures and/or tables and drafted the work or revised it critically for important

299   content.

Competing interest statement

301   All authors declare that they have no competing interests.

Funding statement:

303   This study was funded by the Natural Science Foundation of Shanghai (grant number

304   20ZR1451600) and the Shanghai Municipal Health Bureau Project (grant number 201940439).

305

References:

307   Alicic RZ, Rooney MT, and Tuttle KR. 2017. Diabetic Kidney Disease: Challenges, Progress, and Possibilities. *Clin J*
308   *Am Soc Nephrol* 12:2032-2045.
309   Asanuma K. 2015. [The role of podocyte injury in chronic kidney disease]. *Nihon Rinsho Meneki Gakkai Kaishi*

310   38:26-36.

311   Boaru SG, Borkham-Kamphorst E, Van de Leur E, Lehnen E, Liedtke C, and Weiskirchen R. 2015. NLRP3
312   inflammasome expression is driven by NF-kappaB in cultured hepatocytes. *Biochem Biophys Res Commun*
313   458:700-706.

314   Chang J, Yu Y, Fang Z, He H, Wang D, Teng J, and Yang L. 2020. Long non-coding RNA CDKN2B-AS1 regulates high
315   glucose-induced human mesangial cell injury via regulating the miR-15b-5p/WNT2B axis. *Diabetol Metab*
316   *Syndr* 12:109.

317   Chen HD, Jiang MZ, Zhao YY, Li X, Lan H, Yang WQ, and Lai Y. 2022. Effects of breviscapine on cerebral ischemia-
318   reperfusion injury and intestinal flora imbalance by regulating the TLR4/MyD88/NF-kappaB signaling
319   pathway in rats. *J Ethnopharmacol*:115691.

320   Choudhury D, Tuncel M, and Levi M. 2010. Diabetic nephropathy -- a multifaceted target of new therapies. *Discov*
321   *Med* 10:406-415.

322   Ding J, Wang K, Liu W, She Y, Sun Q, Shi J, Sun H, Wang DC, and Shao F. 2016. Pore-forming activity and structural
323   autoinhibition of the gasdermin family. *Nature* 535:111-116.

324   Dong W, Jia C, Li J, Zhou Y, Luo Y, Liu J, Zhao Z, Zhang J, Lin S, and Chen Y. 2022. Fisetin Attenuates Diabetic
325   Nephropathy-Induced Podocyte Injury by Inhibiting NLRP3 Inflammasome. *Front Pharmacol* 13:783706.

326   El-Aouni C, Herbach N, Blattner SM, Henger A, Rastaldi MP, Jarad G, Miner JH, Moeller MJ, St-Arnaud R, Dedhar S,
327   Holzman LB, Wanke R, and Kretzler M. 2006. Podocyte-specific deletion of integrin-linked kinase results in
328   severe glomerular basement membrane alterations and progressive glomerulosclerosis. *J Am Soc Nephrol*
329   17:1334-1344.

330   Feng H, Zhu X, Tang Y, Fu S, Kong B, and Liu X. 2021. Astragaloside IV ameliorates diabetic nephropathy in db/db
331   mice by inhibiting NLRP3 inflammasomemediated inflammation. *Int J Mol Med* 48.

332   He C, Zhu H, Li H, Zou MH, and Xie Z. 2013. Dissociation of Bcl-2-Beclin1 complex by activated AMPK enhances
333   cardiac autophagy and protects against cardiomyocyte apoptosis in diabetes. *Diabetes* 62:1270-1281.

334   Jefferson JA, Shankland SJ, and Pichler RH. 2008. Proteinuria in diabetic kidney disease: a mechanistic viewpoint.
335   *Kidney Int* 74:22-36.

336   Jian C, Fu J, Cheng X, Shen LJ, Ji YX, Wang X, Pan S, Tian H, Tian S, Liao R, Song K, Wang HP, Zhang X, Wang Y, Huang
337   Z, She ZG, Zhang XJ, Zhu L, and Li H. 2020. Low-Dose Sorafenib Acts as a Mitochondrial Uncoupler and
338   Ameliorates Nonalcoholic Steatohepatitis. *Cell Metab* 31:892-908 e811.

339   Jiang M, Zhao M, Bai M, Lei J, Yuan Y, Huang S, Zhang Y, Ding G, Jia Z, and Zhang A. 2021. SIRT1 Alleviates
340   Aldosterone-Induced Podocyte Injury by Suppressing Mitochondrial Dysfunction and NLRP3
341   Inflammasome Activation. *Kidney Dis (Basel)* 7:293-305.

342   Jiang W, Li Z, Zhao W, Chen H, Wu Y, Wang Y, Shen Z, He J, Chen S, Zhang J, and Fu G. 2016. Breviscapine
343   attenuatted contrast medium-induced nephropathy via PKC/Akt/MAPK signalling in diabetic mice. *Am J*
344   *Transl Res* 8:329-341.

345   Ke G, Chen X, Liao R, Xu L, Zhang L, Zhang H, Kuang S, Du Y, Hu J, Lian Z, Dou C, Zhang Q, Zhao X, Zhang F, Zhu S, Ma
346   J, Li Z, Li S, He C, Wen Y, Feng Z, Zheng M, Lin T, Li R, Li B, Dong W, Chen Y, Wang W, Ye Z, Deng C, Xiao H,
347   Xiao J, Liang X, Shi W, and Liu S. 2021. Receptor activator of NF-kappaB mediates podocyte injury in
348   diabetic nephropathy. *Kidney Int* 100:377-390.

349   Lan T, Jiang S, Zhang J, Weng Q, Yu Y, Li H, Tian S, Ding X, Hu S, Yang Y, Wang W, Wang L, Luo D, Xiao X, Piao S, Zhu
350   Q, Rong X, and Guo J. 2022. Breviscapine alleviates NASH by inhibiting TGF-beta-activated kinase 1-

351 dependent signaling. *Hepatology* 76:155-171.

352 Lasithiotaki I, Tsitoura E, Samara KD, Trachalaki A, Charalambous I, Tzanakis N, and Antoniou KM. 2018.
353 NLRP3/Caspase-1 inflammasome activation is decreased in alveolar macrophages in patients with lung
354 cancer. *PLoS One* 13:e0205242.

355 Latz E, Xiao TS, and Stutz A. 2013. Activation and regulation of the inflammasomes. *Nat Rev Immunol* 13:397-411.

356 Lee JH, Khin PP, Lee G, Lim OK, and Jun HS. 2022. Effect of BBT-877, a novel inhibitor of ATX, on a mouse model of
357 type 1 diabetic nephropathy. *Aging (Albany NY)* 14:6467-6480.

358 Lin J, Cheng A, Cheng K, Deng Q, Zhang S, Lan Z, Wang W, and Chen J. 2020. New Insights into the Mechanisms of
359 Pyroptosis and Implications for Diabetic Kidney Disease. *Int J Mol Sci* 21.

360 Liu T, Zhang L, Joo D, and Sun SC. 2017. NF-kappaB signaling in inflammation. *Signal Transduct Target Ther* 2.

361 Liu WT, Peng FF, Li HY, Chen XW, Gong WQ, Chen WJ, Chen YH, Li PL, Li ST, Xu ZZ, and Long HB. 2016a. Metadherin
362 facilitates podocyte apoptosis in diabetic nephropathy. *Cell Death Dis* 7:e2477.

363 Liu X, Yao L, Sun D, Zhu X, Liu Q, Xu T, and Wang L. 2016b. Effect of breviscapine injection on clinical parameters in
364 diabetic nephropathy: A meta-analysis of randomized controlled trials. *Exp Ther Med* 12:1383-1397.

365 Liu Y, Wen PH, Zhang XX, Dai Y, and He Q. 2018. Breviscapine ameliorates CCl4induced liver injury in mice through
366 inhibiting inflammatory apoptotic response and ROS generation. *Int J Mol Med* 42:755-768.

367 Livak KJ, and Schmittgen TD. 2001. Analysis of relative gene expression data using real-time quantitative PCR and
368 the 2(-Delta Delta C(T)) Method. *Methods* 25:402-408.

369 Lv F, He Y, Xu H, Li Y, Han L, Yan L, Lang H, Zhao Y, Zhao Z, and Qi Y. 2022. CD36 aggravates podocyte injury by
370 activating NLRP3 inflammasome and inhibiting autophagy in lupus nephritis. *Cell Death Dis* 13:729.

371 Mo G, Liu X, Zhong Y, Mo J, Li Z, Li D, Zhang L, and Liu Y. 2021. IP3R1 regulates Ca(2+) transport and pyroptosis
372 through the NLRP3/Caspase-1 pathway in myocardial ischemia/reperfusion injury. *Cell Death Discov* 7:31.

373 Nagata M. 2016. Podocyte injury and its consequences. *Kidney Int* 89:1221-1230.

374 Peng L, Wen L, Shi QF, Gao F, Huang B, Meng J, Hu CP, and Wang CM. 2020. Scutellarin ameliorates pulmonary
375 fibrosis through inhibiting NF-kappaB/NLRP3-mediated epithelial-mesenchymal transition and
376 inflammation. *Cell Death Dis* 11:978.

377 Percie du Sert N, Hurst V, Ahluwalia A, Alam S, Avey MT, Baker M, Browne WJ, Clark A, Cuthill IC, Dirnagl U,
378 Emerson M, Garner P, Holgate ST, Howells DW, Karp NA, Lazic SE, Lidster K, MacCallum CJ, Macleod M,
379 Pearl EJ, Petersen OH, Rawle F, Reynolds P, Rooney K, Sena ES, Silberberg SD, Steckler T, and Wurbel H.
380 2020. The ARRIVE guidelines 2.0: Updated guidelines for reporting animal research. *PLoS Biol*
381 18:e3000410.

382 Qi XM, Wu GZ, Wu YG, Lin H, Shen JJ, and Lin SY. 2006. Renoprotective effect of breviscapine through suppression
383 of renal macrophage recruitment in streptozotocin-induced diabetic rats. *Nephron Exp Nephrol* 104:e147-
384 157.

385 Rousseau M, Denhez B, Spino C, Lizotte F, Guay A, Cote AM, Burger D, and Geraldes P. 2022. Reduction of DUSP4
386 contributes to podocytes oxidative stress, insulin resistance and diabetic nephropathy. *Biochem Biophys*
387 *Res Commun* 624:127-133.

388 Sawaf H, Thomas G, Taliercio JJ, Nakhoul G, Vachharajani TJ, and Mehdi A. 2022. Therapeutic Advances in Diabetic
389 Nephropathy. *J Clin Med* 11.

390 Schena FP, and Gesualdo L. 2005. Pathogenetic mechanisms of diabetic nephropathy. *J Am Soc Nephrol* 16 Suppl
391 1:S30-33.

392 Selby NM, and Taal MW. 2020. An updated overview of diabetic nephropathy: Diagnosis, prognosis, treatment
393   goals and latest guidelines. *Diabetes Obes Metab* 22 Suppl 1:3-15.
394 Shahzad K, Fatima S, Khawaja H, Elwakiel A, Gadi I, Ambreen S, Zimmermann S, Mertens PR, Biemann R, and
395   Isermann B. 2022. Podocyte-specific Nlrp3 inflammasome activation promotes diabetic kidney disease.
396   *Kidney Int* 102:766-779.
397 Shankland SJ. 2006. The podocyte's response to injury: role in proteinuria and glomerulosclerosis. *Kidney Int*
398   69:2131-2147.
399 Shi J, Zhao Y, Wang K, Shi X, Wang Y, Huang H, Zhuang Y, Cai T, Wang F, and Shao F. 2015. Cleavage of GSDMD by
400   inflammatory caspases determines pyroptotic cell death. *Nature* 526:660-665.
401 Song S, Shi C, Bian Y, Yang Z, Mu L, Wu H, Duan H, and Shi Y. 2022. Sestrin2 remedies podocyte injury via
402   orchestrating TSP-1/TGF-beta1/Smad3 axis in diabetic kidney disease. *Cell Death Dis* 13:663.
403 Tang Z, Ji L, Han M, Xie J, Zhong F, Zhang X, Su Q, Yang Z, Liu Z, Gao H, and Jiang G. 2020. Pyroptosis is involved in
404   the inhibitory effect of FL118 on growth and metastasis in colorectal cancer. *Life Sci* 257:118065.
405 Thomas HY, and Ford Versypt AN. 2022. Pathophysiology of mesangial expansion in diabetic nephropathy:
406   mesangial structure, glomerular biomechanics, and biochemical signaling and regulation. *J Biol Eng* 16:19.
407 Tschopp J, and Schroder K. 2010. NLRP3 inflammasome activation: The convergence of multiple signalling
408   pathways on ROS production? *Nat Rev Immunol* 10:210-215.
409 Wang M, Zhang WB, Zhu JH, Fu GS, and Zhou BQ. 2009. Breviscapine ameliorates hypertrophy of cardiomyocytes
410   induced by high glucose in diabetic rats via the PKC signaling pathway. *Acta Pharmacol Sin* 30:1081-1091.
411 Wang MZ, Wang J, Cao DW, Tu Y, Liu BH, Yuan CC, Li H, Fang QJ, Chen JX, Fu Y, Wan BY, Wan ZY, Wan YG, and Wu
412   GW. 2022a. Fucoidan Alleviates Renal Fibrosis in Diabetic Kidney Disease via Inhibition of NLRP3
413   Inflammasome-Mediated Podocyte Pyroptosis. *Front Pharmacol* 13:790937.
414 Wang Y, Cao C, Zhu Y, Fan H, Liu Q, Liu Y, Chen K, Wu Y, Liang S, Li M, Li L, Liu X, Zhang Y, Wu C, Lu G, and Wu M.
415   2022b. TREM2/beta-catenin attenuates NLRP3 inflammasome-mediated macrophage pyroptosis to
416   promote bacterial clearance of pyogenic bacteria. *Cell Death Dis* 13:771.
417 Wolf G. 2004. New insights into the pathophysiology of diabetic nephropathy: from haemodynamics to molecular
418   pathology. *Eur J Clin Invest* 34:785-796.
419 Xu X, Huang X, Zhang L, Qin Z, and Hua F. 2021. Adiponectin protects obesity-related glomerulopathy by inhibiting
420   ROS/NF-kappaB/NLRP3 inflammation pathway. *BMC Nephrol* 22:218.
421 Xu XX, Zhang W, Zhang P, Qi XM, Wu YG, and Shen JJ. 2013. Superior renoprotective effects of the combination of
422   breviscapine with enalapril and its mechanism in diabetic rats. *Phytomedicine* 20:820-827.
423 Yan R, Zhang Y, Yang Y, Liu L, Guo Z, Yu H, Wang Y, and Guo B. 2022. Peroxisome Proliferator-Activated Receptor
424   Gene Knockout Promotes Podocyte Injury in Diabetic Mice. *Biomed Res Int* 2022:9018379.
425 Yang M, and Zhao L. 2022. The Selective NLRP3-Inflammasome Inhibitor CY-09 Ameliorates Kidney Injury in
426   Diabetic Nephropathy by Inhibiting NLRP3-inflammasome Activation. *Curr Med Chem*.
427 Yasuno K, Ishihara S, Saito R, Ishikawa M, Kato T, Kobayashi R, Baba T, Kawano K, Ogihara K, Kamiie J, and Shirota K.
428   2010. Early-onset podocyte injury and glomerular sclerosis in osborne-mendel rats. *J Vet Med Sci* 72:1319-
429   1327.
430 Yu Y, Dong H, Zhang Y, Sun J, Li B, Chen Y, Feng M, Yang X, Gao S, and Jiang W. 2022. MicroRNA-223
431   downregulation promotes HBx-induced podocyte pyroptosis by targeting the NLRP3 inflammasome. *Arch*
432   *Virol* 167:1841-1854.

433 Zhang Q, Hu Y, Hu JE, and Zhang M. 2022a. Solasonine alleviates high glucose-induced podocyte injury through
434   increasing Nrf2-medicated inhibition of NLRP3 activation. *Drug Dev Res*.
435 Zhang T, Wang K, Fan H, Yang Q, Zhang X, Liu F, Feng X, Chen Y, Teng D, Zhao P, and Dong J. 2022b. Ameliorative
436   effect of scutellarin on acute alcohol brain injury in mice. *J Zhejiang Univ Sci B* 23:258-264.
437 Zhong Y, Lee K, Deng Y, Ma Y, Chen Y, Li X, Wei C, Yang S, Wang T, Wong NJ, Muwonge AN, Azeloglu EU, Zhang W,
438   Das B, He JC, and Liu R. 2019. Arctigenin attenuates diabetic kidney disease through the activation of
439   PP2A in podocytes. *Nat Commun* 10:4523.

440

441

442

443

444 **Figure legends**

445 **Figure 1. Bre decreased glomerular injury in DN mice.**

446 (A) The establishment of diabetic mice model and treatment procedure. After being treated with

447 Bre (15 or 30 mg/kg) for 4 weeks, the mice were euthanized, and renal tissues were collected for

448 HE (B, scale bar = 100 μm), PAS (D, scale bar = 50 μm), and Masson (E, scale bar = 50 μm)

449 staining. (C) The glomerular surface area was measured in accordance with the results of HE

450 staining. After being treated with Bre (15 or 30 mg/kg) for 4 weeks, the mice were euthanized,

451 and blood samples were collected to assess serum creatinine (F) and BUN (G) levels. n=7.

452 *$p<0.05$, **$p<0.01$, ***$p<0.001$.

453 **Figure 2. Bre decreased HG-induced podocyte apoptosis *in vitro***

454 After being treated with HG and Bre (50 or 100 μM) for 48 h, MPC5 cell viability (A) and

455 apoptosis (B and C) were assessed using CCK-8 assays and TUNEL staining, respectively. (D)

456 After being treated with HG and Bre (50 or 100 μM) for 48 h, Bax and Bcl-2 protein levels in

457 MPC5 cells were assessed by western blot analysis. (E) Intracellular ROS levels were assessed in

458   MPC5 cells after treatment with HG and Bre (100 μM). **$p<0.01$.

459   **Figure 3. Bre decreased HG-induced podocyte injury *in vitro***

460   After being treated with HG and Bre (50 or 100 μM) for 48 h, the mRNA (A) and protein levels

461   (B and C) of α-SMA, podocin, and synaptopodin were assessed in MPC5 cells using qRT–PCR

462   and western blot analysis, respectively. (D) IF analysis of α-SMA and synaptopodin in MPC5

463   cells after treatment with HG and Bre (50 or 100 μM) for 48 h. **$p<0.01$.

464   **Figure 4. Bre decreased NF-κB/NLRP3-mediated pyroptosis in HG-treated podocytes *in***

465   ***vitro***

466   (A and B) After being treated with HG and Bre (50 or 100 μM) for 48 h, the protein levels of p-

467   p65 were assessed in MPC5 cells by western blot analysis. (C) IF analysis was carried out to

468   assess the nuclear translocation of p65 in MPC5 cells after being treated with HG and Bre (50 or

469   100 μM) for 48 h. (D and E) After being treated with HG and Bre (50 or 100 μM) for 48 h, the

470   protein levels of NLRP3 and activated caspase 1 were assessed in MPC5 cells by western blot

471   analysis. (F) qRT–PCR analysis of IL-18 and IL-1β mRNA levels in MPC5 cells. (G) Western

472   blot analysis of GSDMD protein levels in MPC5 cells. (H) ELISA analysis of LDH release in

473   MPC5 cells. **$p<0.01$.

474   **Figure 5. Bre decreased HG-induced podocyte injury by inhibiting NLRP3-mediated**

475   **pyroptosis *in vitro***

476   (A) After being treated with HG, MCC950 (10 μM), and Ac-YVAD-cmk (40 μM) for 48 h,

477   MPC5 cell viability was assessed using CCK-8 assays. (B) After being treated with HG,

478   MCC950 (10 μM), and Ac-YVAD-cmk (40 μM) for 48 h, the mRNA levels of α-SMA and

479   synaptopodin in MPC5 cells were assessed using qRT–PCR. qRT–PCR (C), western blotting (D

480   and E), and IF (F) analysis were carried out to assess α-SMA and synaptopodin levels in MPC5

481   cells after treatment with nigericin (10 μM) for 48 h in the presence of HG and Bre. **$p<0.01$.

482   **Figure 6. Bre inhibited NLRP3 activation and decreased podocyte injury in the renal**

483   **tissues of DN mice**

484   (A) After being treated with Bre (30 mg/kg) for 4 weeks, the mice were euthanized, and renal

485   tissues were collected to assess synaptopocin expression by IHC analysis. (B) qRT–PCR analysis

486   of α-SMA and podocin mRNA levels in the renal tissues of control mice, DN mice, and Bre-

487   treated mice. (C) After being treated with Bre (30 mg/kg) for 4 weeks, the mice were euthanized,

488   and renal tissues were collected to assess NLRP3 expression by IHC analysis. (D) qRT–PCR

489   analysis of IL-1β, IL-18, TNF-α, and IL-6 mRNA levels in the renal tissues of control mice, DN

490   mice, and Bre-treated mice. **$p<0.01$.

491   **Supporting Figure S1.** ELISA analysis of IL-1β concentration in MPC5 cells supernatant after

492   treatment with HG and Bre (50 or 100 μM) for 48 h. **$p<0.01$.

493

Figure 1

Bre decreased glomerular injury in DN mice.
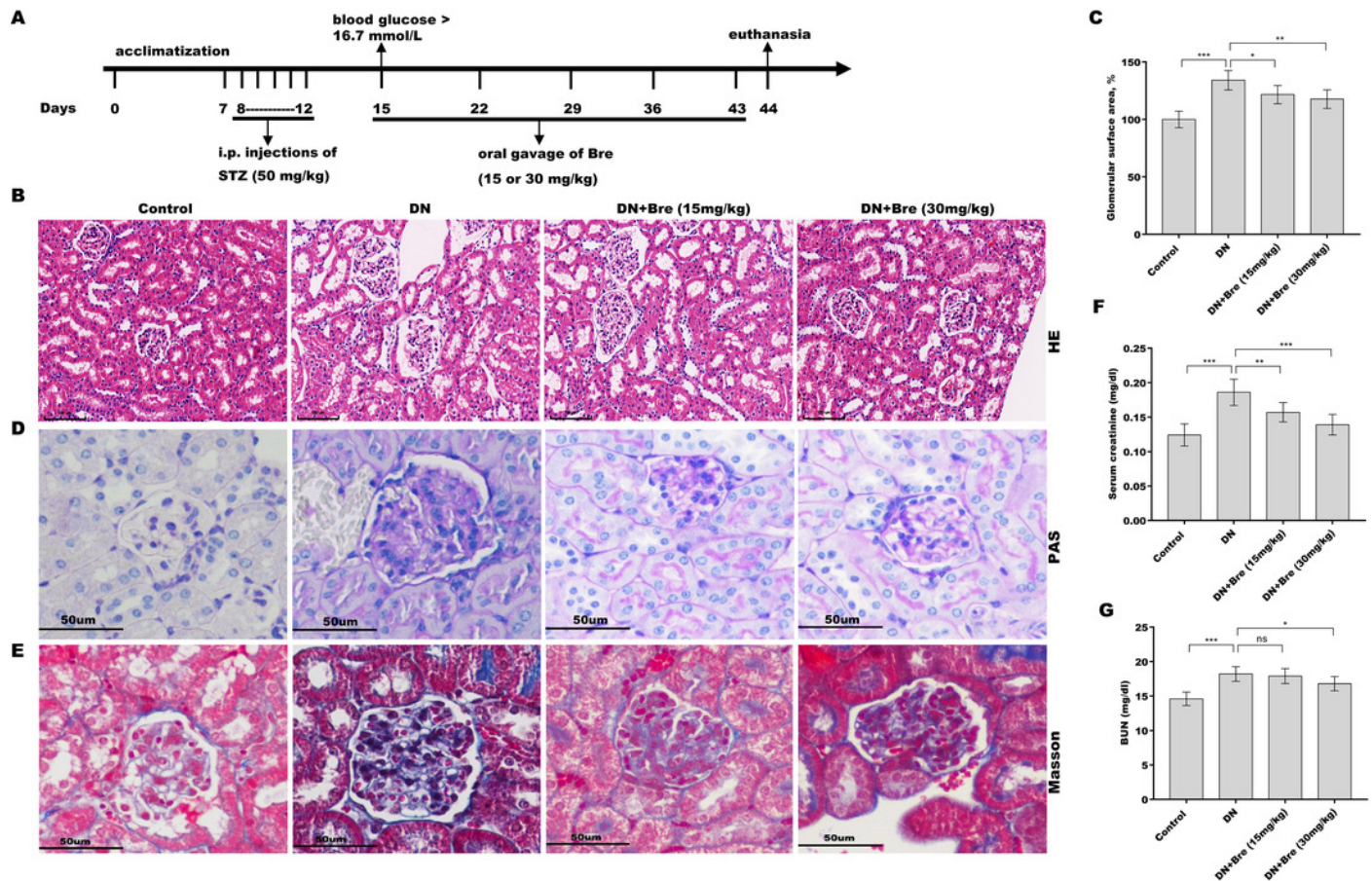
Figure 2

Bre decreased HG-induced podocyte apoptosis *in vitro*
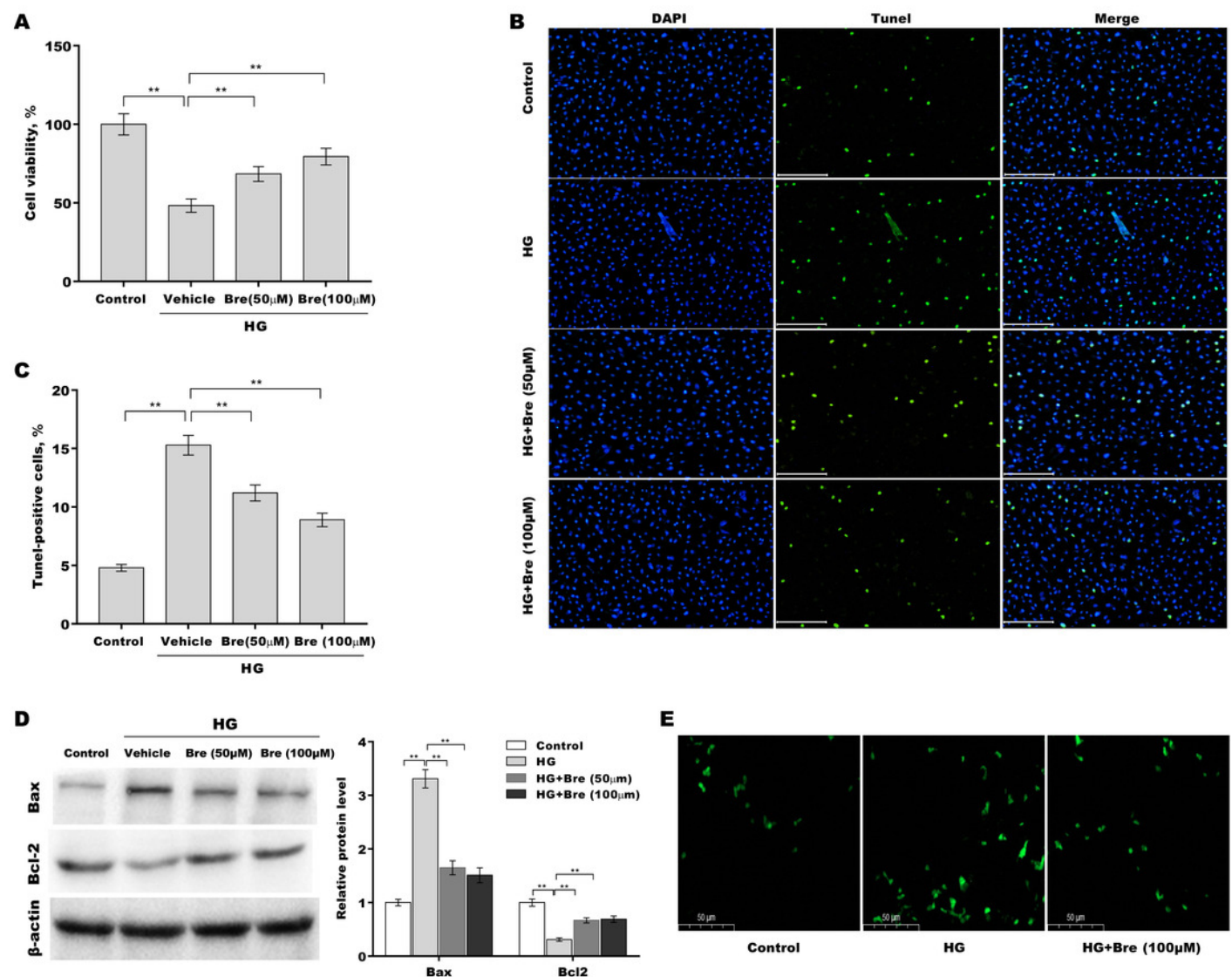
Figure 3

Bre decreased HG-induced podocyte injury *in vitro*
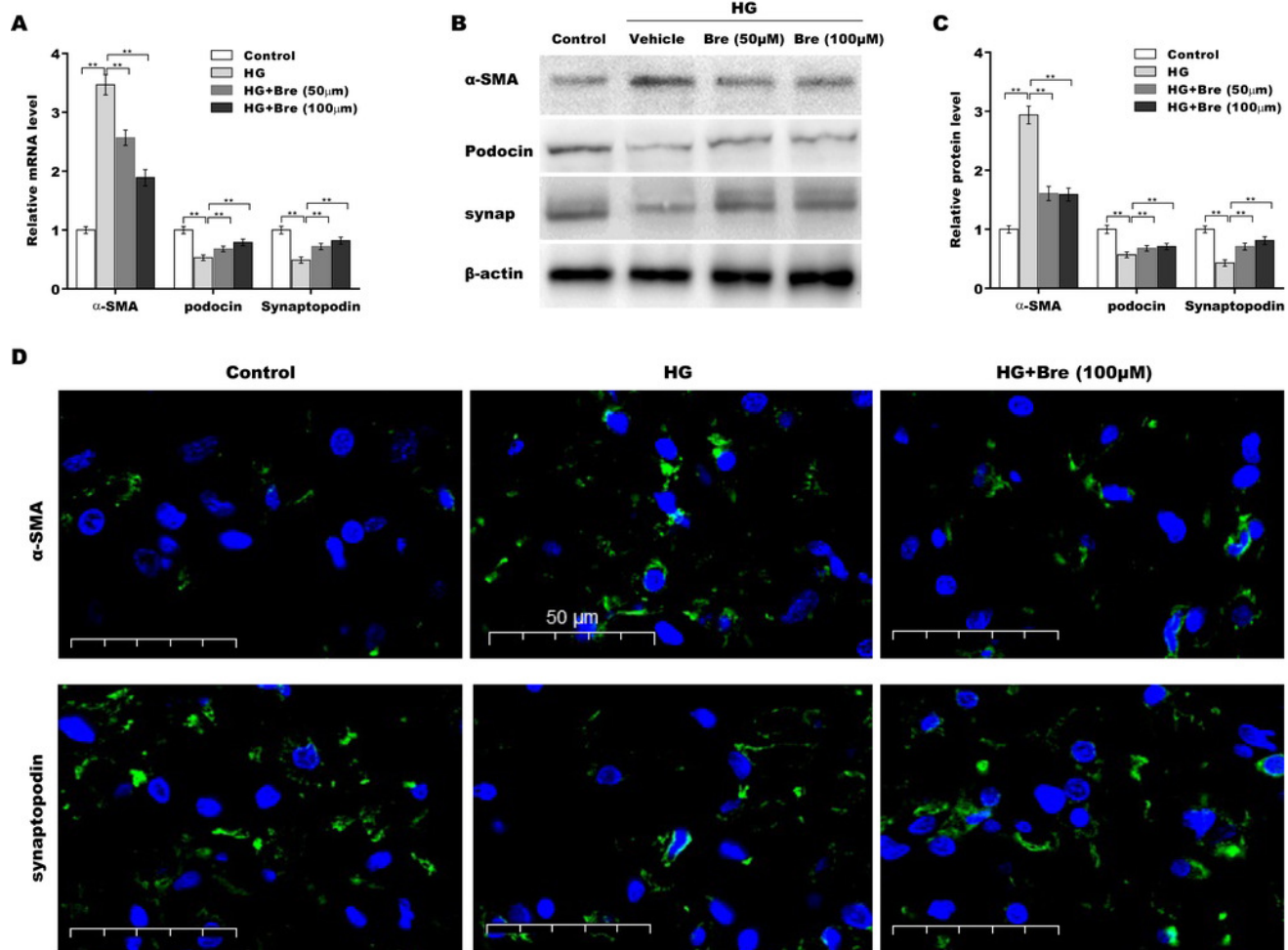
Figure 4

Bre decreased NF-κB/NLRP3-mediated pyroptosis in HG-treated podocytes *in vitro.*
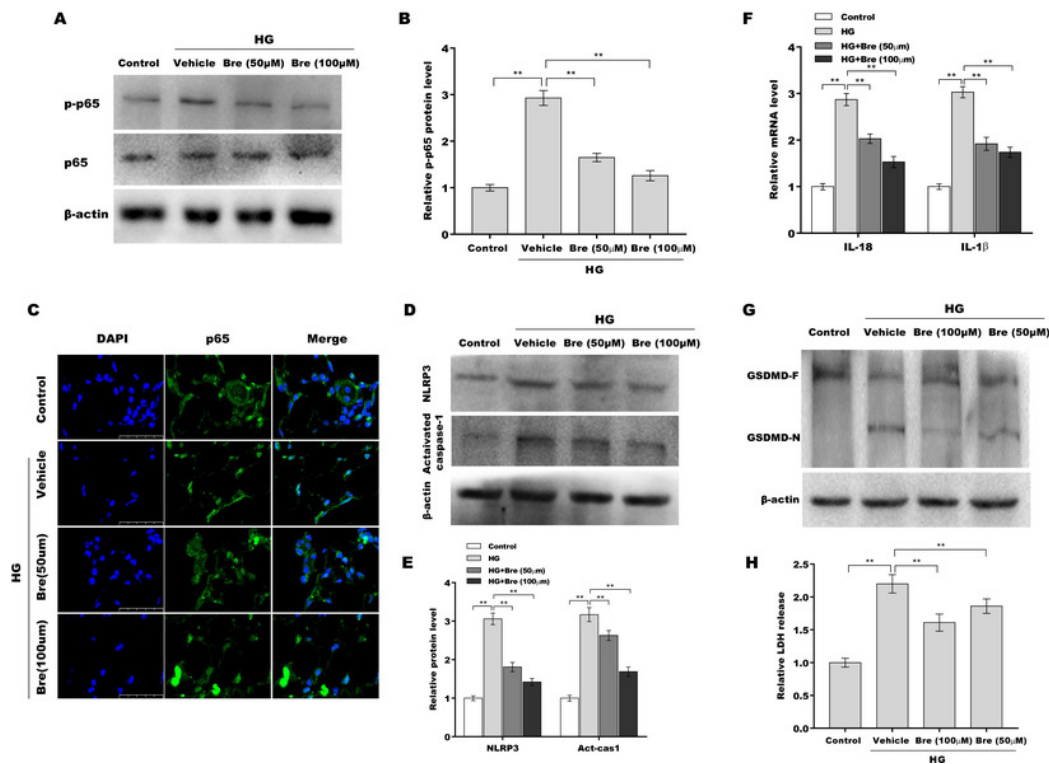
Figure 5

Bre decreased HG-induced podocyte injury by inhibiting NLRP3-mediated pyroptosis *in vitro.*

Figure 6

Bre inhibited NLRP3 activation and decreased podocyte injury in the renal tissues of DN mice.